Variations in onset of action potential broadening: effects on calcium current studied in chick ciliary ganglion neurones

John M. Pattillo, Debra E. Artim, James E. Simples Jr and Stephen D. Meriney

Department of Neuroscience, University of Pittsburgh, Pittsburgh, PA 15260, USA

1. The voltage dependence and kinetic properties of stage 40 ciliary ganglion calcium currents were determined using short (10 ms) voltage steps. These properties aided the interpretation of the action potential-evoked calcium current described below, and the comparison of our data with those observed in other preparations.

2. Three different natural action potential waveforms were modelled by a series of ramps to generate voltage clamp commands. Calcium currents evoked by these model action potentials were compared before and after alterations in the repolarization phase of each action potential.

3. Abrupt step repolarizations from various time points were used to estimate the time course of calcium current activation during each action potential. Calcium current evoked by fast action potentials (duration at half-amplitude, 0·5 or 1·0 ms) did not reach maximal activation until the action potential had repolarized by 40–50 %. In contrast, calcium current evoked by a slow action potential (duration at half-amplitude, 2·2 ms) was maximally activated near the peak of the action potential.

4. Slowing the rate of repolarization of the action potential (broadening) from different times was used to examine effects on peak and total calcium influx. With all three waveforms tested, broadening consistently increased total calcium influx (integral). However, peak calcium current was either increased or decreased depending on the duration of the control action potential tested and the specific timing of the initiation of broadening the repolarization phase.

5. The opposite effects on peak calcium current observed with action potential broadening beginning at different time points in repolarization may provide a mechanism for the variable effects of potassium channel blockers on transmitter release magnitude.

Action potential (AP) invasion of a nerve terminal is the natural stimulus that opens calcium channels critical for neurotransmitter release (Katz, 1969). The magnitude of transmitter released is tightly regulated by the magnitude of calcium entry into the nerve terminal at exocytotic release sites (Llinas *et al.* 1981; Augustine *et al.* 1991). The shape and time course of the AP that depolarizes nerve terminal membrane regulates the gating of calcium channels and the magnitude of the calcium flux. Under physiological conditions, modulation of AP shape and time course can fine tune the magnitude of transmitter released indirectly through changes in calcium influx characteristics (Klein & Kandel, 1980; Spencer *et al.* 1989).

In most preparations, calcium entry during an AP has been shown to begin just after the peak of the AP (Llinas *et al.* 1981; Toth & Miller, 1995; Sabatini & Regehr, 1996; Borst & Sakmann, 1998). The depolarizing phase of the AP initiates calcium channel opening, but the driving force for calcium entry through these open channels is relatively low at the peak of the AP (Llinas *et al.* 1981). Calcium influx increases

during the repolarization of the AP because the open calcium channels pass more calcium ions as the driving force for calcium entry increases. As a result, the speed and magnitude of calcium entry during an AP is very sensitive to the time course of the repolarization phase of the AP.

Potassium channels are important because they shape the repolarization and after-hyperpolarization (AHP) phases of the AP. Blockade or inactivation of voltage-gated potassium channels has been shown to cause AP broadening that results in increased calcium influx and transmitter release (Augustine, 1990; Wheeler *et al.* 1996; Sabatini & Regehr, 1997). Calcium-activated potassium (BK) channels are of particular interest because they have been shown to be co-localized with calcium channels in the active zone (Roberts *et al.* 1990; Robitaille *et al.* 1993), and can contribute to repolarization during a single AP (Lindgren & Moore, 1989; Roberts *et al.* 1990; Lancaster *et al.* 1991; Solaro *et al.* 1995; Yazejian *et al.* 1997). Blockade of BK channels has been shown to broaden somal APs at various times during AP repolarization and/or decrease the size of the AHP (Adams

et al. 1982; Storm, 1987; Sah & McLachlan, 1992; Solaro *et al.* 1995; Zhang & McBain, 1995; Davies *et al.* 1996).

At the synapse, BK channel blockade or *slowpoke* gene mutation has been shown to either increase (Robitaille & Charlton, 1992) or decrease (Warbington *et al.* 1996; Pattillo & Meriney, 1997) transmitter release magnitude. A decrease in transmitter release magnitude resulting from a decrease in peak calcium influx has also been reported following AP broadening in the jellyfish, where these effects are attributed to A-type potassium current inactivation (Spencer *et al.* 1989). These opposite effects on transmitter release may result from subtle differences in the precise timing of effects on AP broadening and/or differences in BK and calcium channel gating.

This work was initiated to enhance our understanding of the conditions under which the balance of influences that regulate calcium entry during APs is dominated by calcium channel activation or the driving force for calcium entry. We have examined the balance between these influences on peak and total calcium influx using three different types of AP waveforms. We have estimated the time course of calcium channel activation during each type of AP and measured the effects of broadening the repolarization phase from different points in the time course of the AP. The time at which driving force becomes the dominant influence depends on the normal shape of the AP, because the time course of calcium channel activation is different with APs of differing shapes.

METHODS

Cell culture

Ciliary ganglia were dissected from White Leghorn chicken embryos (quickly decapitated) at stage 40 (Hamburger & Hamilton, 1951) in Tyrode solution containing (mM): 134 NaCl, 3 KCl, 3 CaCl$_2$, 1 MgCl$_2$, 12 glucose and 20 NaH$_2$CO$_3$, pH 7·2. Ganglia were incubated sequentially in collagenase (0·5 mg ml^{-1}) and trypsin (0·08%) in Ca^{2+}- and Mg^{2+}-free Tyrode solution for 20 min each. Trypsin was removed and inhibited by three washes in minimal essential medium (MEM) plus 10% heat-inactivated horse serum. Ganglia were dissociated mechanically by gentle trituration through a polished Pasteur pipette. The final suspension of cells was centrifuged at 100 *g* for 5 min and resuspended in MEM plus 10% chick embryo extract. Cells were plated onto poly-D-lysine-coated 35 mm plastic dishes, incubated at 37 °C, and used for experiments after 1–6 h of incubation.

Whole cell patch-clamp recordings

The traditional whole cell patch-clamp method was used for all experiments (Hamill *et al.* 1981). To isolate calcium currents, we bathed cells in an external saline of the following composition (mM): 140 or 100 NaCl, 10 or 50 TEA-Cl, 10 Hepes, 5 glucose, 5 KCl, 5 CaCl$_2$ and 2 MgCl$_2$ plus 1 μM tetrodotoxin, pH 7·3. Pipettes were pulled on a Flaming/Brown Micropipette Puller (Sutter Instruments Co.; Model P-97), coated with Sylgard (Dow Corning), and fire polished (electrode resistances ranged from 0·5 to 2 MΩ). Pipettes were filled with the following internal solution (mM): 120 CsCl, 10 Hepes, 11 EGTA, 5 TEA-Cl, 1 CaCl$_2$ and 4 MgCl$_2$, with 4 Mg-ATP, 0·3 Na-GTP and 0·1 leupeptin added fresh daily. Access

resistance was usually 3–4 MΩ. Before all recordings, we corrected for the $-4\cdot3$ mV liquid junction potential. Series resistance was compensated by 80–90%. Currents were activated, acquired and leak-subtracted using a hyperpolarizng *P*/4 protocol by the pCLAMP software package (Axon Instruments) running on a Pentium processor-based microcomputer in concert with an Axopatch 200A patch-clamp amplifier (Axon Instruments). Voltage dependence and kinetics of ciliary ganglion calcium currents were determined using 10 ms voltage steps from -80 mV to potentials between -50 and $+60$ mV. After stepping back to -80 mV, the peak of the tail current was used as an estimate of the steady-state activation of calcium currents and these data were fitted with a Boltzmann function. To determine the time constant for activation of calcium currents, the calcium current was fitted to a single exponential beginning when inward current crossed baseline. To determine the time constant for deactivation, the decay of tail currents to baseline was fitted with a single exponential beginning 80 μs after the peak of the tail current.

The APs used in the construction of model AP waveforms were adapted from Borst *et al.* (1995) and Brody *et al.* (1997) for the calyx of Held AP, and from unpublished observations (J. M. Pattillo, J. E. Simples & S. D. Meriney) for the motoneurone AP and the ciliary ganglion AP. The AHP was removed from the modelled AP waveforms since it did not affect significantly the peak calcium influx and only slightly affected the very late phases of total calcium influx (see Fig. 6). Further, removing the AHP simplified alterations to the repolarization phase. Our descriptions of the time when alterations of the repolarization phase were begun are relative to the peak of the AP, defined as that time point at the end of the short plateau phase of the peak. Calcium currents were four-pole Bessel filtered at 5 kHz and digitized at 20 kHz. An average of four to six currents were used for all comparisons. Calcium currents activated by altered APs were compared with a control recording taken within 30 s of the experimental recording to control for the effects of calcium current run-down. Furthermore, the order in which the broadening protocols were used was varied so that any potential error due to run-down would be minimized. The total calcium influx was measured as the integral of the calcium current bounded by the time point at which inward current initially deviated from baseline, and the time at which it returned to baseline. Nifedipine (RBI) was solubilized in DMSO at 1 mM and diluted into bath saline to 1 μM. All other reagents were obtained from Sigma and dissolved in saline. All values are expressed as means $\pm$ S.E.M. and all cells were studied at room temperature (22–23 °C).

RESULTS

Calcium current in ciliary ganglion neurones

Below we have examined the time course of calcium channel activation during different AP waveforms, and the effects of AP broadening on calcium current. To aid in the interpretation of these data and to facilitate comparison with other studies, we have examined the voltage dependence of calcium current activation and the kinetics of calcium current activation and deactivation using traditional square voltage step commands (Fig. 1). Stage 40 ciliary ganglion neuronal somata express predominantly N-type calcium channels (White *et al.* 1997). These currents began to activate at about -40 mV and maximal current flowed at about 0 mV (Fig. 1*A–C*). A Boltzmann fit of the steady-

state activation curve indicates half-maximal activation at −4 mV (Fig. 1*B*). Activation and deactivation time constants are known to be voltage dependent (Hodgkin & Huxley, 1952). To estimate the speed of calcium current activation over the voltage range that is relevant to the AP waveforms used below, we fitted (using a single exponential) the activation of calcium currents in response to voltage steps between −10 and +30 mV (O, Fig. 1*D*). To estimate the speed of calcium current deactivation over the voltage range relevant to the AP waveforms used below, we fitted (using a single exponential) the deactivation of tail currents following a repolarization step from +30 mV (peak of our AP waveforms) to between −20 and −60 mV (●, Fig. 1*D*).

Action potential waveforms

Three APs were selected to represent a wide range of AP durations present in neurones. The fastest AP examined ('fast') had a duration at half-amplitude of approximately

0·5 ms and was adapted from a study of the calyx of Held (Borst *et al.* 1995). The maximum slope of the rising phase of the fast AP was 308 mV ms^{-1}. The second AP ('medium') was obtained from our recordings of APs in the presynaptic varicosities of *Xenopus* motoneurones in culture (J. M. Pattillo & S. D. Meriney, unpublished observations). This AP had a duration at half-amplitude of 1 ms and a maximum rising phase slope of 94 mV ms^{-1}. The slowest AP examined ('slow'), with a duration at half-amplitude of 2·2 ms and a maximum rising phase slope of 83 mV ms^{-1}, was taken from our recordings of APs in cultured chick ciliary ganglion neurones (J. E. Simples & S. D. Meriney, unpublished observations). These three AP waveforms were faithfully modelled with a series of voltage ramps (4–5) up to and including the small plateau at the peak (Fig. 2). However, the repolarizing phase was simplified to a single ramp to allow for consistent modification. To isolate the effects of changing AP shape such that they included only changes in
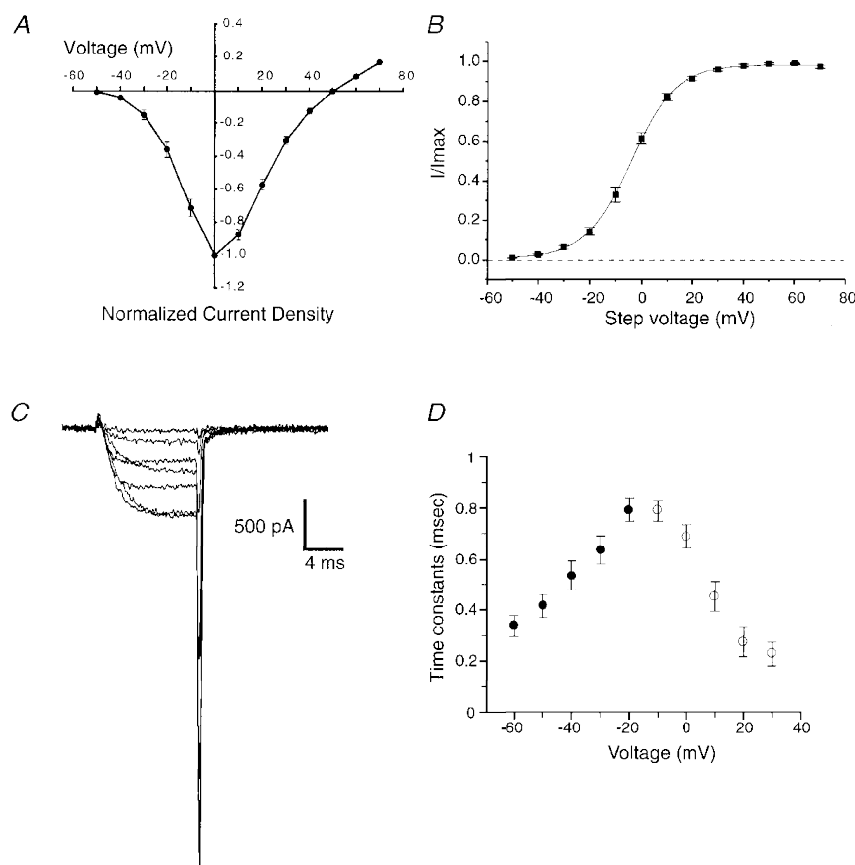

Figure 1. Properties of calcium current in stage 40 ciliary ganglion neurones

A, current–voltage relationship obtained from six representative cells. To facilitate pooling of data from cells of different size, raw current amplitude values were divided by the capacitance recorded from each cell to obtain a current density (pA pF^{-1}) and these were normalized to the largest value from each cell. *B*, voltage dependence of activation obtained by plotting normalized tail current amplitude (I/I_{max}) against the step potential used to activate current (means ± s.e.m.; $n = 6$). The continuous line represents a Boltzmann fit to the data. *C*, representative family of currents elicited by voltage steps between −30 and +30 mV in 10 mV increments ($V_{hold} = -80$ mV). *D*, time constants for calcium current activation (O) and deactivation (●) at voltages to which calcium channels are exposed during AP waveforms (means ± s.e.m.; $n = 6$).

repolarization, all of the model APs were scaled in the voltage dimension so that they had a resting potential of −60 mV and a peak amplitude of +30 mV. This is within 5 mV of the actual values for resting and peak potentials for the native APs on which the models were based, with the exception of the calyx of Held AP (natural resting potential = −80 mV; Borst *et al.* 1995). The three model AP waveforms derived from the calyx of Held, *Xenopus* motoneurone varicosities and chick ciliary ganglion neurones will be referred to as the fast, medium and slow AP, respectively, from here forward.

Calcium current activation during an action potential

To gain an understanding of the time course of calcium current activation during the repolarizing phase of different APs, we divided the repolarizing phase into several time points at which the voltage command was stepped back to −80 mV (Fig. 3*A* and *B*). The peak of the resulting tail current was taken as a relative estimation of calcium channel activation at that point in the AP.

When the fast AP waveform was examined, the peak of calcium current activation occurred 230 μs after the peak of the AP when the membrane potential had reached −15 mV, which corresponded to 50% of AP repolarization (Fig. 3*C* and *D*). The fast AP was so brief that even when the voltage returned to baseline (−60 mV), calcium current was still 75% of maximum activation. The peak calcium current activation during the medium AP occurred 400 μs after the peak of the AP when the membrane potential had reached −6 mV, corresponding to 40% of AP repolarization (Fig. 3*C* and *D*). The slower rate of repolarization of the medium AP allowed for significant deactivation of calcium current to occur as the membrane potential approached baseline. Thus, when repolarization was complete, calcium activation was only 38% of maximum (Fig. 3*C* and *D*). The slow AP waveform elicited a calcium current that was near maximal at the peak of the AP. Calcium current activation peaked

400 μs after the peak of the AP, when the membrane potential had only repolarized to +21 mV (10% of AP repolarization). Calcium current activation during the slow AP appeared to plateau until the membrane potential dropped to below +5 mV, at which point deactivation began to reduce the number of active calcium channels. The slow repolarization rate of this AP allowed for calcium current to almost completely deactivate before the membrane potential reached baseline.

The ciliary ganglion neurones that were used for these experiments express both N- and L-type calcium channels, but N-type channels constitute about 75% of the total calcium current at this developmental stage (White *et al.* 1997). For some experiments using the slow and medium AP waveforms, nifedipine (1 μM) was added to the bath to block L-type calcium channels. In these experiments, there was no significant difference in the calcium current activation curves when compared with those collected in the absence of nifedipine (data not shown). Thus, although the data presented here reflect the effects of AP waveform alterations on both N- and L-type calcium channels, removal of the relatively minor L-type channel contribution did not significantly alter the data.

Timing of action potential broadening

To examine the effect of variations in the onset of AP broadening, we increased the duration of each of the AP waveforms by 1 ms, and varied the point in the repolarization at which the increase in duration began (Fig. 4). The peak and integral of the elicited calcium currents were then compared with those elicited by a control AP waveform.

The effect of AP broadening on the peak calcium current was dependent on the timing of the AP broadening. Broadening of the fast AP beginning at the peak of the AP caused the peak of the elicited calcium current to increase
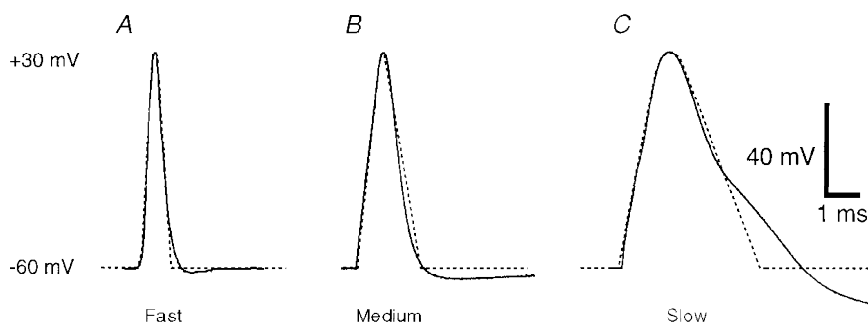

Figure 2. Action potential waveforms

To create the fast, medium, and slow model AP waveforms, three natural APs (continuous lines) of different durations were used. APs were adapted from the presynaptic terminal of the calyx of Held (*A*), the presynaptic *Xenopus* motoneurone varicosity (*B*) and the soma of a chick ciliary ganglion neurone (*C*). To facilitate the use of these as voltage-clamp commands, the rising phase was modelled using a series of ramps (dotted lines), and the falling phase was simplified to a single ramp to allow consistent alterations in the repolarization phase. The APs were normalized to a resting potential of −60 mV and a peak amplitude of +30 mV.
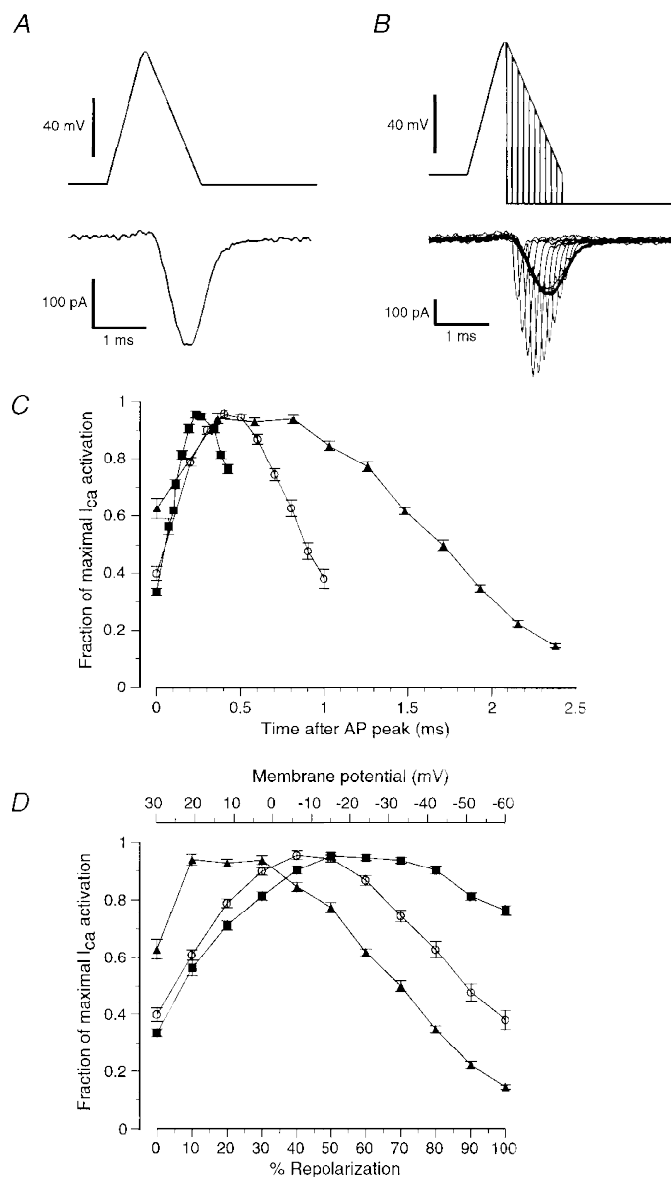
Figure 3. Estimation of the timing of calcium current activation during an AP waveform

A, control calcium current evoked by the medium AP waveform. *B*, family of tail currents (thin lines) evoked by instantaneous repolarizations of the medium AP waveform to −80 mV at various times during the AP repolarization. The amplitudes of these tail currents were used to estimate the relative number of calcium channels that were open at each point in the repolarization. *C* and *D*, summary of data obtained with the protocol outlined in *B* using the three different AP waveforms (fast AP (■); medium AP (O); slow AP (▲); means ± s.e.m.; *n* > 16). *C*, depending on the specific AP waveform tested, maximal calcium channel activation occurred at different times following the peak of the AP waveform. Each point represents a normalized ratio of the amplitude of the tail current evoked by the repolarization steps to −80 mV compared with the amplitude of a control AP waveform evoked current (thick line in *B*). The fractional activation was calculated by setting the maximum ratio in each cell to 1, and expressing the remaining ratios as fractions of 1. *D*, same data as in *C*, but plotted with membrane potential (top) or percentage AP repolarization (bottom) on the *x*-axis instead of time. When the slow AP was used, calcium current activation was maximal soon after the peak of the AP (+21 mV; 10% of repolarization; ▲). For the medium AP, calcium current activation was maximal at about −6 mV, or 40% of repolarization (O). For the fast AP, calcium current activation did not become maximal until about −15 mV, or at about 50% of AP repolarization (■).

by $21 \pm 2\%$ relative to the control fast AP (Fig. 4Aa). However, when broadening was delayed to a point when repolarization was 20% complete, a small decrease in the peak of the calcium current was observed. Broadening from later time points further decreased the peak amplitude of the calcium current (Fig. 5A, ■). The greatest decrease in peak calcium current was $27 \pm 1\%$, which occurred when broadening was delayed to a point when repolarization was 50% complete (Figs 4Ab and 5A). The effect of broadening on peak calcium current diminished as the time at which broadening began was delayed to 60% of repolarization or greater (Fig. 5A). In contrast to the effects of broadening on peak calcium current, broadening from any point led to increases in the total calcium influx (integral) relative to control (Fig. 5B, ■). This effect diminished steadily as

broadening was delayed to later points in the repolarizing phase of the AP waveform. When the onset of broadening was delayed until 20% of repolarization or later, the increases in integral were largely confined to the latter half of the calcium influx (Fig. 4Ab).

Broadening of the medium AP had a similar effect on peak calcium current (Figs 4B and 5, ○). Broadening of the AP from the peak led to an $8 \pm 4\%$ increase in peak calcium current. The effect of broadening on peak calcium current reversed when broadening was delayed to a point when repolarization was 10% complete. The maximum decrease in peak calcium current of $19 \pm 0.4\%$ was observed when broadening was delayed until repolarization was 40% complete (Figs 4Bb and 5A). When broadening was delayed until later points in repolarization, the effect on peak
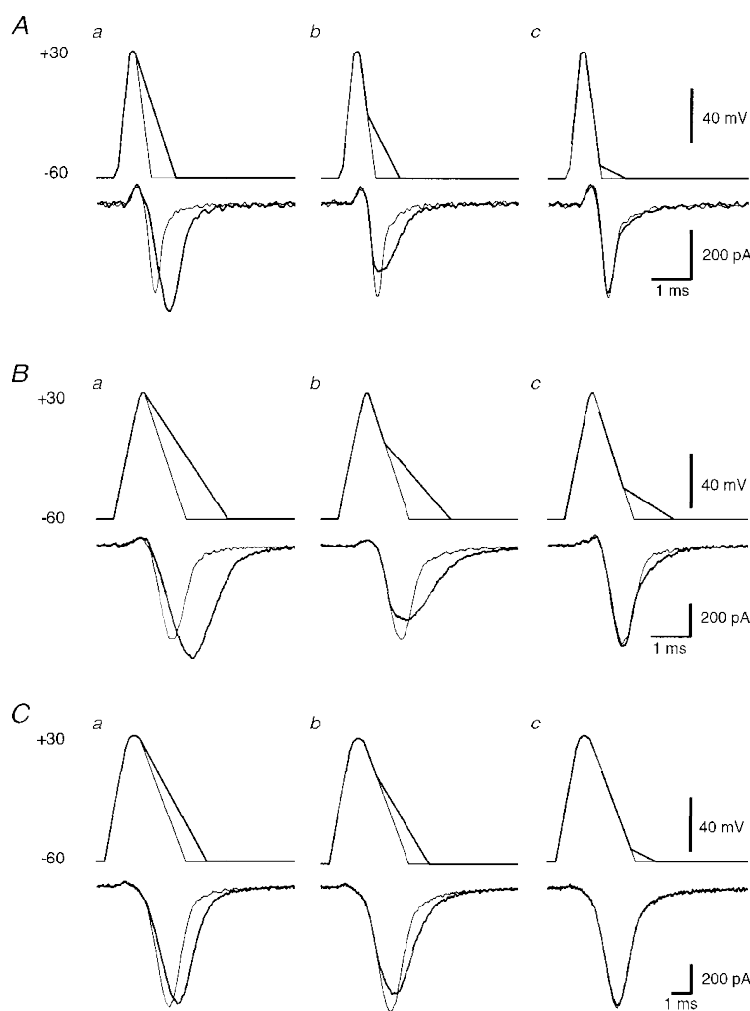

Figure 4. Effects on calcium current of broadening each of three AP waveforms at different times during repolarization

In all cases, the control AP and associated calcium current are shown using thin lines. Broadened APs and associated calcium currents are shown using thick lines. A, fast AP broadened from the peak (a), 50% of repolarization (b) and 90% of repolarization (c). B, medium AP broadened from the peak (a), 40% of repolarization (b) and 75% of repolarization (c). C, slow AP broadened from the peak (a), 30% of repolarization (b) and 90% of repolarization (c). Example AP waveforms chosen for panel b in A–C were selected to represent maximal reductions in peak calcium current.

calcium current diminished. As with the fast AP, broadening from any point caused an increase in the integral of calcium current (Fig. 5*B*). The increase in total calcium influx (integral) was largely confined to the later phases of the AP-evoked calcium influx (Fig. 4*Bb*).

In contrast to the effects of broadening using the fast or medium APs, broadening of the slow AP from the peak resulted in a decrease in the peak of the evoked calcium current ($6 \pm 1\%$; Figs 4*Ca* and 5*A*, ▲). This decrease in peak calcium current was most prominent ($12 \pm 1\%$) when broadening was delayed until repolarization was 30% complete (Figs 4*Cb* and 5*A*). The effect of broadening on the peak of the AP-evoked current diminished when broadening was delayed to 40% of repolarization or greater. As with the fast and medium APs, broadening of the slow AP from any point in the repolarizing phase resulted in an increase in the integral of the calcium current (Fig. 5*B*).

DISCUSSION

Calcium current during an AP will be determined by the balance between the number of open channels, the time the channels reside in the open state and the electrochemical driving force present when the channels are open. Any change in the shape of the AP will affect calcium current depending on the timing of that change and the specific balance of these three influences at that point in the AP. We have shown that the time course of activation of calcium current during an AP varies depending on the duration of the AP. In all three AP waveforms tested, the activation of calcium channels was not complete at the peak of the AP, but continued into repolarization. Depending on the AP waveform tested, calcium channel activation was maximal at between 10 and 50% of repolarization. Furthermore, the fast AP was so brief that, in the second half of repolarization, very little channel deactivation occurred. This may have been due to the unnatural abruptness of the repolarization in our simplified AP waveforms. Nevertheless, a significant number of channels remaining open when the membrane potential reaches baseline suggests that changes in the amplitude of the AHP might play a role in the regulation of calcium influx during very brief APs. To test this hypothesis, we added a 5 mV AHP to the fast AP by linearly extending the repolarization phase to −65 mV (Fig. 6). The presence or absence of this 5 mV model AHP did not change significantly the magnitude of the peak calcium current. This may be due to the balanced contribution of increased driving force and

Figure 5. Summary of the effects of AP broadening on the three AP waveforms tested

A, broadening of the three different AP waveforms had different effects on peak calcium current. Broadening the slow AP, in which calcium current activation had been shown to be maximal near the peak of the AP, only resulted in decreases in peak calcium influx (▲). Broadening the medium AP resulted in increases in peak calcium current when the broadening began before 10% of AP repolarization (+21 mV), but in decreases in peak calcium current when it began later than 10% of repolarization (○). Maximal decreases in peak calcium current resulted from broadening that began when the AP had repolarized by about 40% (−6 mV). Broadening the fast AP resulted in increases in peak calcium current when the broadening began before 20% of AP repolarization (+12 mV), but decreases in peak calcium current when it began later than 20% of repolarization (■). Maximal decreases in peak calcium current resulted from broadening that began when the AP had repolarized by about 50% (−15 mV). *B*, broadening AP waveforms always increased the total calcium influx (measured as the integral) independent of when AP broadening began (except at very late phases of the AP, where there were no significant effects). All values are the mean ± S.E.M. ($n > 14$).
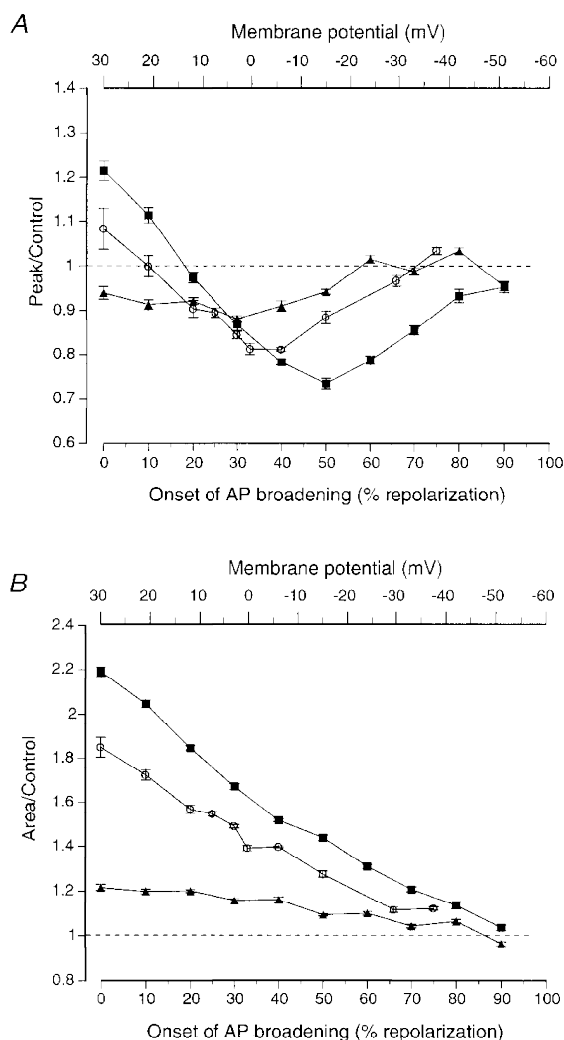
faster calcium channel deactivation. The addition of an AHP did cause a small decrease in the late phases of total calcium influx that was most probably due to more rapid calcium channel deactivation at this more hyperpolarized potential. It should be noted that all of the experiments reported here were performed at room temperature. At physiological temperatures, calcium channels would be expected to gate more rapidly and shift the time of maximal activation during AP repolarization to earlier in the AP waveform (Sabatini & Regehr, 1996). Additionally, the small charge screening effect of using 5 mM calcium, instead of the more physiological 2 mM, might also shift the time course of calcium channel gating slightly during an AP.

The differences in the time course of calcium current activation during the repolarizing phase of the three different APs used here are reflected in the effect on calcium current of variations in the onset of AP broadening. During the slow AP, calcium current activation was maximal soon after the peak of the AP. Thus, any AP broadening would not be likely to open more calcium channels, but would have its effects predominantly by decreasing the electrochemical driving force for calcium and delaying calcium channel deactivation. This is supported by the observation that broadening the slow AP beginning at the peak resulted in a decrease in peak calcium current and an increase in the integral of calcium current. During faster APs, broadening from the peak might be expected to cause the opening of more calcium channels (Augustine, 1990). Since calcium current activation did not peak until the AP had repolarized by 40% for the medium AP and 50% for the fast AP, broadening these APs increased peak calcium current until the broadening began at 20% of repolarization or later. In fact, maximal decreases in peak calcium current occurred when broadening began near the time when calcium current activation had reached a maximum (40 and 50% of repolarization for medium and fast APs, respectively). Broadening-induced decreases in peak calcium current became less dramatic when broadening began very late in

the AP repolarization, as driving force differences between the control AP and the broadened AP were diminished.

Regardless of the time of onset, AP broadening always increased the integral of calcium current in all three APs tested. When the two fastest APs were broadened beginning near the peak, the increase in the integral of calcium current observed can be explained as a combination of the effects of increased calcium channel activation and slowing of calcium channel deactivation. Broadening from later points where calcium current activation was maximal, or near maximal, led to an increase in the integral of calcium current primarily by slowing the deactivation of calcium channels. In the slow AP, where calcium current activation was maximal near the peak, increases in total calcium influx resulting from broadening AP repolarization were most likely to have been caused primarily by slowing of calcium channel deactivation.

Although our model APs allowed us to examine the effects of varying the onset of AP broadening during repolarization, they are not intended to reflect the precise time course of modifications seen in native neurone APs. Selective BK channel blockade usually causes broadening that increases in magnitude as repolarization of the AP progresses and is not the linear function modelled here. This difference will certainly alter the specific timing of when AP broadening causes an increase or decrease in peak calcium current, but not the general principle discussed here.

There are two possible mechanisms that could underlie an increase in peak calcium current following AP broadening. Single APs have been shown to effectively open the majority of available calcium channels (Borst & Sakmann, 1998), but the maximal activation of calcium channels during a brief AP does not occur until well after the peak of the AP (Fig. 3). Therefore, by decreasing the rate of repolarization, AP broadening could slow calcium channel deactivation and cause maximal calcium channel activation to occur closer to the peak of the AP. This would result in a greater number of
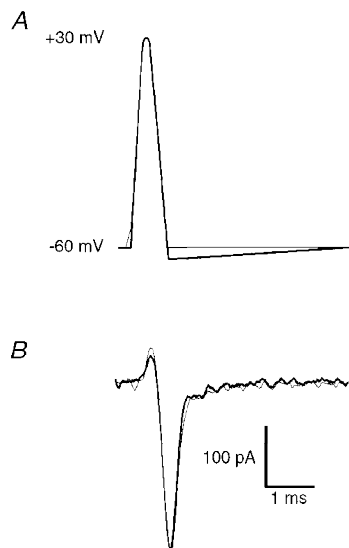

Figure 6. Effects on calcium current of an AHP following the fast AP waveform

Extension of the repolarization phase of the fast AP by 5 mV below the resting potential of −60 mV (model AHP) had little or no effect on calcium current. *A*, model AP waveforms used to evoke calcium current. *B*, calcium currents evoked by control AP (thin line) and AP with added model AHP (thick line).

open calcium channels contributing to the peak of the calcium current. Alternatively, if an AP does not activate all of the available calcium channels (Pumplin *et al.* 1981), AP broadening could open additional calcium channels, resulting in increased peak calcium current (Augustine, 1990).

Numerous studies have demonstrated that blockade of potassium channels leads to AP broadening. Application of potassium channel blockers that target voltage-gated potassium channels, or non-specific potassium channel blockers that target both voltage-gated and large-conductance calcium-activated potassium channels, typically results in broadening beginning at the peak of the AP (Augustine, 1990; Sabatini & Regehr, 1996; Wheeler *et al.* 1996). However, specific blockade of large-conductance calcium-activated potassium channels can result in AP broadening beginning at various times during repolarization (Storm, 1987; Sah & McLachlan, 1992; Solaro *et al.* 1995; Zhang & McBain, 1995; Davies *et al.* 1996). These effects are observed in many types of neurones with AP shapes that vary from fast time course APs in central interneurones (Zhang & McBain, 1995) to much slower APs in peripheral ganglion neurones and chromaffin cells (Solaro *et al.* 1995; Davies *et al.* 1996).

The effects of AP broadening have also been examined with reference to the magnitude of transmitter released and have been shown to be variable depending on the preparation examined. Blockade of voltage-gated potassium channels increases the magnitude of transmitter release in many preparations (Klein & Kandel, 1980; Llinas *et al.* 1981; Coates & Bullock, 1985; Gainer *et al.* 1986; Augustine, 1990; Wheeler *et al.* 1996; Sabatini & Regher, 1996). Interestingly, inactivation of A-type potassium currents has been shown to decrease transmitter release in jellyfish neurones (Spencer *et al.* 1989). Selective BK channel blockade has been shown to increase transmitter release at adult neuromuscular synapses (Robitaille *et al.* 1993), but decrease transmitter release at cultured embryonic neuromuscular synapses (Pattillo & Meriney, 1997). The mutation of the *slowpoke* gene in *Drosophila* (which codes for a BK channel) also decreases the magnitude of transmitter release (Warbington *et al.* 1996). These contrasting effects may result from variability in the timing of when these potassium channels contribute to the AP waveform. In neuronal somata, BK channels have been shown to be tightly coupled to specific types of calcium channels (Wisgirda & Dryer, 1994; Davies *et al.* 1996). Alterations in the precise coupling of BK channels to calcium channels, or the modulation of BK channel properties, would be expected to alter the timing of their contribution to AP repolarization.

The increases or decreases in transmitter release outlined above that result from blockade, inactivation, or mutation of potassium channels suggest that AP broadening at transmitter release sites can either increase or decrease the calcium influx that is relevant to the regulation of transmitter release magnitude. Our data demonstrate that AP broadening invariably increases the total calcium influx

(integral), but can have opposite effects on peak calcium current depending on the timing of broadening. The specific aspect of calcium influx (rate of influx or total calcium entry) that is most relevant to transmitter release magnitude may depend on the specific arrangement of calcium channels and docked vesicles at the synapse. Release of docked neurotransmitter vesicles is thought to be triggered by the intracellular microdomain of high calcium concentration near the mouth of active zone calcium channels (Chad & Eckert, 1984; Fogelson & Zucker, 1985; Simon & Llinas, 1985; Bertram *et al.* 1996; Naraghi & Neher, 1997). The largest and most transient changes in $[Ca^{2+}]_i$ occur near the mouth of the channel. At sites further away from the mouth of the channel, $[Ca^{2+}]_i$ rises more slowly to an elevated level (Augustine *et al.* 1991). The large transient very close to the mouth of a calcium channel may be the most sensitive to small changes in the instantaneous driving force. Thus, release sites that are sensing calcium very near this large transient may be the most sensitive to the potentially opposite effects on the rate of calcium influx caused by AP broadening from different points in the repolarization.

The subtle control over the time course of AP repolarization is an important point of regulation over calcium influx and transmitter release. The influences that determine the consequences of alterations in potassium channel contribution to transmitter release regulation probably include the duration of the AP, the kinetics of calcium and potassium channel activation and deactivation, and the relationship between presynaptic calcium channels and the transmitter release apparatus.

ADAMS, P. R., CONSTANTI, A., BROWN, D. A. & CLARK, R. B. (1982). Intracellular Ca^{2+} activates a fast voltage-sensitive K^+ current in vertebrate sympathetic neurones. *Nature* **296**, 746–749.

AUGUSTINE, G. J. (1990). Regulation of transmitter release at the squid giant synapse by presynaptic delayed rectifier potassium current. *Journal of Physiology* **431**, 343–364.

AUGUSTINE, G. J., ADLER, E. M. & CHARLTON, M. P. (1991). The calcium signal for transmitter secretion from presynaptic nerve terminals. *Annals of the New York Academy of Sciences* **635**, 365–381.

BERTRAM, R., SHERMAN, A. & STANLEY, E. F. (1996). Single-domain/bound calcium hypothesis of transmitter release and facilitation. *Journal of Neurophysiology* **75**, 1919–1931.

BORST, J. G., HELMCHEN, F. & SAKMANN, B. (1995). Pre- and postsynaptic whole-cell recordings in the medial nucleus of the trapazoid body of the rat. *Journal of Physiology* **489**, 825–840.

BORST, J. G. G. & SAKMANN, B. (1998). Calcium current during a single action potential in a large presynaptic terminal of the rat brainstem. *Journal of Physiology* **506**, 143–157.

BRODY, D. L., PATIL, P. G., MULLE, J. G., SNUTCH, T. P. & YUE, D. T. (1997). Bursts of action potential waveforms relieve G-protein inhibition of recombinant P/Q-type Ca^{2+} channels in HEK 293 cells. *Journal of Physiology* **499**, 637–644.

CHAD, J. E. & ECKERT, R. (1984). Calcium domains associated with individual channels can account for anomalous voltage relations of Ca-dependent responses. *Biophysical Journal* **45**, 993–999.

COATES, C. J. & BULLOCK, G. M. (1985). Synaptic plasticity in the Molluscan peripheral nervous system: physiology and role of peptides. *Journal of Neuroscience* **5**, 2677–2684.

DAVIES, P. J., IRELAND, D. R. & McLACHLAN, E. M. (1996). Sources of Ca^{2+} for different Ca^{2+}-activated K^+ conductances in neurones of the rat superior cervical ganglion. *Journal of Physiology* **495**, 353–366.

FOGELSON, A. L. & ZUCKER, R. S. (1985). Presynaptic calcium diffusion from various arrays of single channels. Implications for transmitter release and synaptic facilitation. *Biophysical Journal* **48**, 1003–1017.

GAINER, H., WOLFE, S. A. J., OBAID, A. L. & SALZBERG, B. M. (1986). Action potentials and frequency-dependent secretion in the mouse neurohypophysis. *Neuroendocrinology* **43**, 557–563.

HAMBURGER, V. & HAMILTON, H. L. (1951). A series of normal stages in the development of the chick embryo. *Journal of Morphology* **88**, 49–92.

HAMILL, O. P., MARTY, A., NEHER, E., SAKMANN, B. & SIGWORTH, F. J. (1981). Improved patch-clamp techniques for high-resolution current recording from cells and cell-free membrane patches. *Pflügers Archiv* **391**, 85–100.

HODGKIN, A. L. & HUXLEY, A. F. (1952). A quantitative description of membrane current and its application to conductance and excitation in nerve. *Journal of Physiology* **117**, 500–544.

KATZ, B. (1969). *The Release of Neural Transmitter Substances.* Liverpool University Press, UK.

KLEIN, M. & KANDEL, E. R. (1980). Mechanism of calcium current modulation underlying presynaptic facilitation and behavioral sensitization in *Aplysia. Proceedings of the National Academy of Sciences of the USA* **77**, 6912–6916.

LANCASTER, B., NICOLL, R. A. & PERKEL, D. J. (1991). Calcium activates two types of potassium channels in rat hippocampal neurons in culture. *Journal of Neuroscience* **11**, 23–30.

LINDGREN, C. A. & MOORE, J. W. (1989). Identification of ionic currents at presynaptic nerve endings of the lizard. *Journal of Physiology* **414**, 201–222.

LLINAS, R., STEINBERG, I. Z. & WALTON, K. (1981). Relationship between presynaptic calcium current and postsynaptic potential in squid giant synapse. *Biophysical Journal* **33**, 289–321.

NARAGHI, M. & NEHER, E. (1997). Linearized buffered Ca^{2+} diffusion in microdomains and its implications for calculation of $[Ca^{2+}]$ at the mouth of a calcium channel. *Journal of Neuroscience* **17**, 6961–6973.

PATTILLO, J. M. & MERINEY, S. D. (1997). Iberiotoxin decreases transmitter release at an embryonic neuromuscular junction. *Society for Neuroscience Abstracts* **23**, 2275.

PUMPLIN, D. W., REESE, T. S. & LLINAS, R. (1981). Are the presynaptic membrane particles the calcium channels? *Proceedings of the National Academy of Sciences of the USA* **78**, 7210–7213.

ROBERTS, W. M., JACOBS, R. A. & HUDSPETH, A. J. (1990). Colocalization of ion channels involved in frequency selectivity and synaptic transmission at presynaptic active zones of hair cells. *Journal of Neuroscience* **10**, 3664–3684.

ROBITAILLE, R. & CHARLTON, M. P. (1992). Presynaptic calcium signals and transmitter release are modulated by calcium-activated potassium channels. *Journal of Neuroscience* **12**, 297–305.

ROBITAILLE, R., GARCIA, M. L., KACZOROWSKI, G. J. & CHARLTON, M. P. (1993). Functional colocalization of calcium and calcium-gated potassium channels in control of transmitter release. *Neuron* **11**, 645–655.

SABATINI, B. L. & REGEHR, W. G. (1996). Timing of neurotransmission at fast synapses in the mammalian brain. *Nature* **384**, 170–172.

SABATINI, B. L. & REGEHR, W. G. (1997). Control of neurotransmitter release by presynaptic waveform at the granule cell to Purkinje cell synapse. *Journal of Neuroscience* **17**, 3425–3435.

SAH, P. & McLACHLAN, E. M. (1992). Potassium currents contributing to action potential repolarization and the afterhyperpolarization in rat vagal motoneurons. *Journal of Neurophysiology* **68**, 1834–1841.

SIMON, S. M. & LLINAS, R. R. (1985). Compartmentalization of the submembrane calcium activity during calcium influx and its significance in transmitter release. *Biophysical Journal* **48**, 485–98.

SOLARO, C. R., PRAKRIYA, M., DING, J. P. & LINGLE, C. J. (1995). Inactivating and noninactivating Ca^{2+}- and voltage-dependent K^+ current in rat adrenal chromaffin cells. *Journal of Neuroscience* **15**, 6110–6123.

SPENCER, A. N., PRZYSIEZNIAK, J., ACOSTA-URQUIDI, J. & BASARSKY, T. A. (1989). Presynaptic spike broadening reduces junctional potential amplitude. *Nature* **340**, 636–638.

STORM, J. F. (1987). Action potential repolarization and a fast after-hyperpolarization in rat hippocampal pyramidal cells. *Journal of Physiology* **385**, 733–759.

TOTH, P. T. & MILLER, R. J. (1995). Calcium and sodium currents evoked by action potential waveforms in rat sympathetic neurones. *Journal of Physiology* **485**, 43–57.

WARBINGTON, L., HILLMAN, T., ADAMS, C. & STERN, M. (1996). Reduced transmitter release conferred by mutations in the slowpoke-encoded Ca^{2+}-activated K^+ channel gene of *Drosophila. Invertebrate Neuroscience* **2**, 51–60.

WHEELER, D. B., RANDALL, A. & TSIEN, R. W. (1996). Changes in action potential duration alter reliance of excitatory synaptic transmission on multiple types of Ca^{2+} channels in rat hippocampus. *Journal of Neuroscience* **16**, 2226–2237.

WHITE, M. G., CRUMLING, M. A. & MERINEY, S. D. (1997). Developmental changes in calcium current pharmacology and somatostatin inhibition of calcium current in chick parasympathetic neurons. *Journal of Neuroscience* **17**, 6302–6313.

WISGIRDA, M. E. & DRYER, S. E. (1994). Functional dependence of Ca^{2+}-activated K^+ current on L- and N-type Ca^{2+} channels: differences between chicken sympathetic and parasympathetic neurons suggest different regulatory mechanisms. *Proceedings of the National Academy of Sciences of the USA* **91**, 2858–2862.

YAZEJIAN, B., DiGREGORIO, D. A., VERGARA, J. L., POAGE, R. E., MERINEY, S. D. & GRINNELL, A. D. (1997). Direct measurements of presynaptic calcium and calcium-activated potassium currents regulating neurotransmitter release at cultured *Xenopus* nerve–muscle synapses. *Journal of Neuroscience* **17**, 2990–3001.

ZHANG, L. & McBAIN, C. J. (1995). Potassium conductances underlying repolarization and after-hyperpolarization in rat CA1 hippocampal interneurones. *Journal of Physiology* **488**, 661–672.

Corresponding author

S. D. Meriney: Department of Neuroscience, University of Pittsburgh, 446 Crawford Hall, Pittsburgh, PA 15260, USA.

Email: meriney@bns.pitt.edu